Properties and technical characteristics of Casira pottery, Jujuy, Argentina

***A. Paltrinieri*[1,2]**, *M. F. Serra*[1,2]*, *M. S. Conconi*[1,3]*, *N. M. Rendtorff*[1,3]

[1]Centro de Tecnología de Recursos Minerales y Cerámica, CONICET La Plata, CIC PBA, UNLP,
Camino Centenario y 506, C.C. 49, M. B. Gonnet, Buenos Aires, Argentina
[2]Universidad Nacional de La Plata, Facultad de Artes, La Plata, Buenos Aires, Argentina
[3]Universidad Nacional de La Plata, Facultad de Ciencias Exactas, La Plata, Buenos Aires, Argentina

Abstract

In this work, the results of a multi-technique characterization of a type of pottery production with high cultural and economic relevance from the only potter town in Argentina are presented and correlated. Raw materials, a prepared paste, and ceramic samples were studied. Chemical, structural, textural, microstructural, and thermal features were assessed and described in terms of the raw materials characteristics, fabrication, and firing conditions. Some distinctive properties of this Casira ceramic production, like the thermal expansion coefficient and other technological properties, are reported for the first time. This allowed the establishment of characteristic behaviors of the ceramics under study, which also constitute the basis for their traceability.

Keywords: popular ceramics, Casira, Argentina, properties.

INTRODUCTION

The Argentine northwest and the south of Bolivia constitute a macro-region, historically inhabited by societies with extensive/vast ceramic production. These people are indigenous peasants and migrant populations in mountain areas with production for self-consumption and regional exchange [1, 2]. Pre-Hispanic pottery has been studied from archeology to approximate its cultural complexity. The material culture of the Yavi-Chicha style has been associated with a long period of time: 500 BC to Spanish contact [3-6]; ceramic manufacture changes and continuities occurred during the colonial period [7]. These ceramics were generally used for cooking and serving food. This employment linked to food is observed both in daily activities and in local rituals and festivities in which it is given functions of high symbolic value, such as those used for the preparation, storage, and distribution of 'chicha' [8]. In this region, there is a coexistence with locally made ceramic pieces that determines a very close relationship with this materiality, as well as a type of object characteristic of this territory [9]. Nowadays, the region's pottery production is constituted as a production of handcraft objects with high circulation and economic volume of public sale to tourism then used in urban areas. Ceramic production occurs in an artisanal or semi-artisan way, in small domestic workshops [10].

Although there are several ceramic production centers in Argentina, Casira stands out as the main producer, with other similar ones in Bolivia, but not in Argentina. The town of Casira is located in the Puna region almost on the border with Bolivia, 50 km west of the city of La Quiaca in the department of Cienaguillas, in Jujuy Province. It is located at more than 3500 m above sea level. About 500 people live in the town and there are more than 30 pottery workshops whose production is commercialized throughout the province and even in other provinces of Argentina. Within the ceramics of Casira, there are various utilitarian containers of various uses. The typical pots are known as cantaros, tinajas, virques, floreros, jarras, platos, mecheros, poroñas, candelabras, and taranchas (Fig. 1) [9, 11]. The size of the pots and jars ranges from small pieces of a few centimeters in size to pieces of more than 60 cm in diameter. The operational chain has been previously described [12]. Two raw materials from the area near the town are used: Barro Chico (BC) and Pirka (P) [13], while the first is already in powder, the second must be ground with a hammer mill. The moistening or filling is carried out directly and the dosage is done empirically in a very low ratio of BC. In any case, the ratio between Pirka and BC is greater than 9:1. The shaping methods are varied, generally in the plastic state, and include pinching, slabs construction, the potter's wheel, and filling of plaster molds by pressing in the plastic state [14]. Some workshops have ventured into the casting of slip in plaster molds. A very light slip is usually applied before polishing or burnishing the almost completely dry pieces with the help of smooth stones [7]. The pieces are dried in the open air and fired by two methods, in the open land with guano and in ascending draft wood ovens built with local mud-grass mixtures (adobe*)* and using firewood and/or guano as fuel. The firewood used is remnants of the lumber industry (corner posts) of the southeastern area of the Province of Jujuy or discarded wood pallets [7].

In this work, we intend to describe aspects of the manufacture of high-value ceramic pieces produced in Casira, Argentina. We also pretend to establish the distinctive behavior in drying, heat treatment (firing), and its technical properties, which infer suitable conditions for its culinary

---

**aguspaltrinieri@yahoo.com.ar*
https://orcid.org/0000-0003-3967-2229

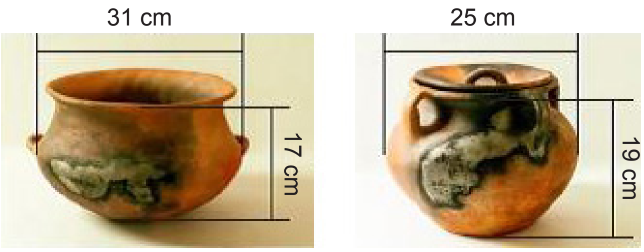

Figure 1: Typical pots (*ollas*) of Casira: a) two-handle pot without lid; and b) four-handle pot with a lid.

use and its relationship with some characteristics of the raw materials and the climatic conditions of the region, and also to establish traceability criteria for these productions, which would be of interest about the protection and promotion of this pottery as a cultural heritage of the region.

MATERIALS AND METHODS

Raw materials, generally used by local producers in Casira, Argentina [12, 13], were studied: Barro Chico (BC) and Pirka (P) clays. A prepared paste (PP) and specimens obtained from a ceramic representative of the production of Casira (CM) were also analyzed. The PP was made of a mixture of BC and P. A multi-technique approach was carried out; Table I shows the performed characterizations, and the actual experimental conditions are shown below. Pirka clay is employed as a temper and the sized grains become of importance, afterward, both plasticity and drying behavior become important for the prepared paste; plastic BC clay plasticity was also studied. The thermal behavior of both raw materials was assessed in order to understand the thermochemical processes and to complement the X-ray diffraction (XRD) analysis for phase identification; scanning electron microscopy (SEM) was performed in the raw materials as well. A systematic dynamic sintering study of the dried PP was performed in order to understand the firing behavior of the sample. Finally, the immersion test is usually employed in order to describe the textural properties of the ceramic material; this was performed on the ceramic sample elaborated by the local ceramic manufacturer; this was complemented with the intrusion mercury porosimetry test in order to obtain a pore size distribution; the microstructure features of the ceramic were finally studied by scanning electron microscopy.

Powder samples (ground to 200 mesh) were analyzed, using a diffractometer (mod. 3020, Philips), with CuKα radiation (λ=1.54 Å) and Ni filter at 35 kV and 40 mA. This was performed in the 2θ range from 3° to 70° in steps of 0.02° (2θ) and 2 s/step. A voltage of 35 kV and a current of 40 mA were used. The identification of the crystalline phases was carried out by comparing the diffraction patterns obtained experimentally with those stored in the database of the International Center for Diffraction Data: Powder Diffraction File-2 (ICDD PDF-2). Microstructural analysis was carried out by scanning electron microscopy (SEM). Samples were coated with carbon and examined using a microscope (JCM 6000 Plus, Jeol). A voltage of 15 kV and a BEI detector were employed. The grain size distribution of the coarse raw material was evaluated in a 500 g batch through 5 standard sieves 10, 20, 50, 100, and 200 mesh in a Rotap type sifter for 10 min. The plasticity of the prepared clay paste (PP) and the fine clay (BC) were evaluated (it was not possible to evaluate the Pirka material since it was a coarse-grained soil that did not present plasticity). Plasticity was established by the relationship between the plastic limit (Atterberg method) and the liquid limit (Casagrande method of 25 strokes and 12 mm joint) [15]. The drying of the humidified plastic clay pastes was evaluated utilizing systematic contraction-mass curves as a function of the mass under ambient conditions; Bigot-type curves were built and 5.00x3.00x0.50 cm^3 samples were employed. The thermochemical processes of the prepared paste were evaluated by thermogravimetric and differential thermal analysis (TG-DTA) using a thermal analyzer (Thermo Plus EVO2 TG 8121, Rigaku). The program used consisted of heating at 10 °C/min up to 1050 °C; an alumina reference sample and platinum crucibles were employed in an air atmosphere.

The heating behavior of the green bodies was studied: green bodies were analyzed by dilatometry (Thermo Evo

Table I - Performed characterization techniques for each studied sample.

Technique	BC	P	PP	CM
Mineralogical characterization (XRD)	X	X		X
Grain size distribution (sieving)		X		
Plasticity (Atterberg method)	X		X	
Drying behavior (Bigot type curve)			X	
Differential thermal analysis-thermogravimetry (DTA-TG)	X	X		
Dilatometry (vertical)			X	X
Water immersion test				X
Mercury intrusion porosimetry				X
Microstructural characterization by scanning electron microscopy (SEM)	X	X		X

BC: Barro Chico clay; P: Pirka clay; PP: prepared paste; CM: ceramic.

Plus II, Rigaku). Six heating programs were established with different maximum temperatures, recording both the heating process (at a speed of 10 °C/min) and the cooling process (10 °C/min). The maximum temperatures reached in this reversible dilatometry were 400, 600, 700, 800, 900, and 1000 °C in the air atmosphere. The phase analysis of the ceramics was carried out under the same conditions as the raw materials, on ground powders (200 mesh) of the ceramics. The open porosity and apparent density of the ceramic were established by the Archimedes immersion method (ASTM C373-88-2006) on 10 fragments of each ceramic piece. Pore size distribution was evaluated by mercury intrusion porosimetry (Pascal 440, Thermoscientific) in the macro and mesopore ranges. Subsequently, the microstructure of the ceramic was observed using a scanning electron microscope (JCM 6000 Plus, Jeol) on a fresh carbon-coated fracture sample. Finally, the dilatometric behavior and thermal expansion coefficient of prepared paste fired at 800 °C were studied. It was carried out in a dilatometer (Thermo, Rigaku) at 500 °C under reversible conditions in an air atmosphere.

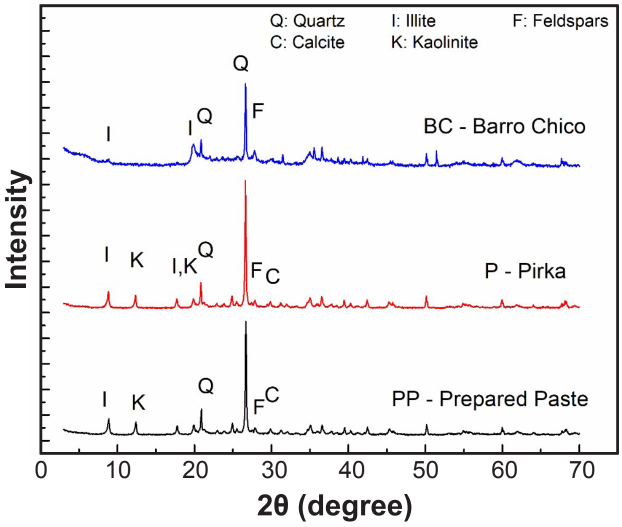

Figure 2: XRD patterns of the raw materials (BC and P) and the prepared paste (PP).

RESULTS

Raw material properties

Mineralogical analysis: the raw materials used by local producers were studied by X-ray diffraction; both powders were ground at 200 mesh to perform the characterization. Diffraction patterns are shown in Fig. 2 and semi-quantitative results are shown in Table II; as expected, both raw materials were clays accompanied by quartz and other accessory minerals. In the case of BC, the clays were smectitic, accompanied by chlorites and illites; the accessory minerals were mainly plagioclase and sanidine, that is, two feldspars, in terms of ceramic behavior [16]. Finally, it is worth mentioning that a trace of an iron phase attributable to hematite was identified. In the case of P powder, the clays were mainly kaolinite and muscovite, within the accessory minerals plagioclase and sanidine were also observed; this raw material also presented a low amount of calcite ($CaCO_3$). It should be noted that this minor phase allowed the approximation of firing temperatures, due to its decomposition [17-19], which would happen at ~780 °C.

Morphology and characteristics of the raw materials studied: Fig. 3 shows scanning electron microscopy images of the raw materials (BC and P) without more mechanical treatment than that used by the producers. An expected degree of agglomeration was observed in both powders; in the BC sample, fine material (few micrometers) and agglomerates or coarse particles (20-50 µm) were observed. In the micrograph, some structures of the phyllosilicate type were observed that corresponded to the XRD results of clays. In the P sample, thicker particles were devised. These were above 50 µm. These particles were accompanied by

Table II - Results of powder X-ray diffraction analysis of the raw materials, prepared paste, and ceramic studied (M: majority; m: minority; t: trace).

Material	Formula	Mineral	Barro Chico (BC)	Pirka Molida (P)	Prepared paste (PP)	Ceramic
SiO_2	SiO_2	Quartz	M	M	M	M
Clay	$K[Al_4Si_2O_9(OH)_3]$	Muscovite/illite	M	m	m	m
	$Al_2Si_2O_5(OH)_4$	Kaolinite	-	M	M	-
	-	Smectite	M	-	m	-
	$(Mg_5Al)(Si,Al)_4O_{10}(OH)_8$	Clinochlore	m	-	m	-
Feldspar	$KAlSi_3O_8$	Sanidine	m	m	m	m
	$NaAlSi_3O_8$	Plagioclase	m	m	m	m
Oxide	TiO_2	Anatase	-	-	-	m
	$CaCO_3$	Calcite	m	m	m	m
	Fe_2O_3	Hematite	t	-	t	t

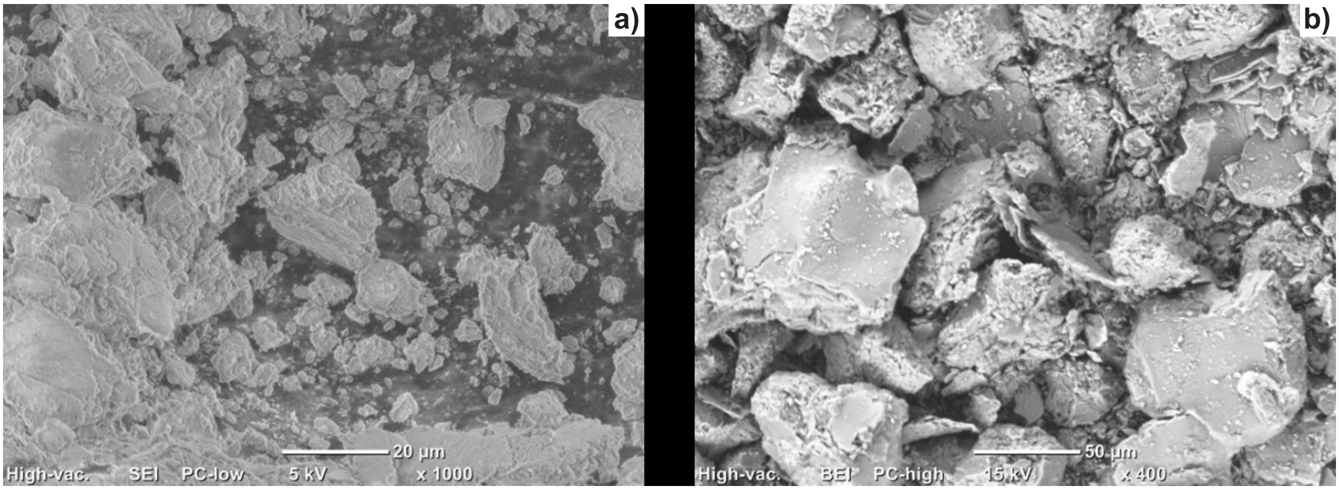

Figure 3: SEM images of the as-employed clays: a) Barro Chico (BC); and b) Pirka (P).

fine powders (<2 µm). The coarse grains presented a higher compaction grade, evidencing a higher cementation grade. Laminar structures were observed in some of the finer grains. These corresponded to phyllosilicate typical structures. Quartz particles cannot be seen or identified in these images, although it was identified by XRD.

Grain size distribution of the Pirka clay: BC powder was under 200 mesh, while P powder was a coarse one, and that is the reason why a granulometric study was carried out with standard sieves. Table III shows the proportion of the different granulometry, displaying a wide distribution below 10 mesh. With just over 15 wt% of fines (below 200 mesh), 26 wt% of particles were between 100 and 200 mesh, and 17 wt% was retained on a 50 mesh sieve. These large particles were observed by microscopic analysis (Fig. 3). A proportion of Pirka grains can be defined as sands or even gravel. The granulometry of this raw material was distinctive and more similar to the granulometry of a refractory than of pottery clay [20].

Table III - Grain size distribution of the Pirka (P) clay.

Standard mesh	Size (µm)	Mass proportion (%)
16	710-1190	17.18
25	297-710	16.52
50	149-297	17.61
100	74-149	26.24
200	≤74	15.15

Thermal behavior analysis of the raw materials: thermogravimetric (TG) and differential thermal analysis (DTA) of the raw materials (BC and P) were carried out, which results are shown in Figs. 4 and 5, respectively; pulverized samples were employed in all the cases. The thermal mass loss of the BC sample showed three steps (Fig. 4b): firstly, a significant loss of 9 wt% occurred below 150 °C, attributable to losses of surface and inter-particle water. Then a wide process between 200 and 400 °C of approximately 2 wt% loss occurred, followed by a more abrupt loss between 450 and 600 °C of 3 wt% reaching a total mass loss of 14 wt%. These were attributable to the structural decompositions of the clays (from the mineralogical point of view) present in the sample. The thermal analysis (Fig. 5b) confirmed that the first process was endothermic, then the second process was exothermic [21, 22] and the last one was endothermic. The exothermic process may be due to organic material combustion or transformation of Fe in clays while de mass loss between 450 and 600 °C corresponded to the typical behavior of the clays. On the DTA curve at 573 °C, a slight signal corresponding to the quartz transformation was observed [23].

The thermogravimetry curve of sample P also showed three steps, although the third was split into two processes (Fig. 4a). The first loss of surface water (<2%) below 100 °C followed by a more abrupt loss at 270 °C of 1%, attributable to the decomposition of Al or Fe hydroxides [22], and the most important loss of mass (from 2.5% to 7%) that started at 500 °C and ended near 700 °C. As mentioned, this step was divided into two stages that were not easy to delimit in the TG curve, which corresponded to the decomposition of clays [24]; both kaolinite and the minority muscovite present this process in this temperature range [25, 26], giving rise to a phase of low crystallinity by dehydroxylation, of the metakaolinite type [27-29]. It should be noted that more losses corresponding to the decomposition of carbonates cannot be observed in this analysis; this corresponded to the low proportion observed in the XRD [21]. Differential thermal analysis (DTA) showed that the three observed processes were endothermic (centered at 48, 261, and 509 ºC, Fig. 5a). The transformation corresponding to the transformation of quartz was seen in this sample as well. Observable as slight shoulder in the DTA (centered at 568 ºC). Finally, an exothermic peak close to 980 °C was clearly observed, which corresponded to the transformation of metakaolinite to the spinel phase of the alumina-silica system, observable in kaolinitic clays [25, 27, 30, 31]. The

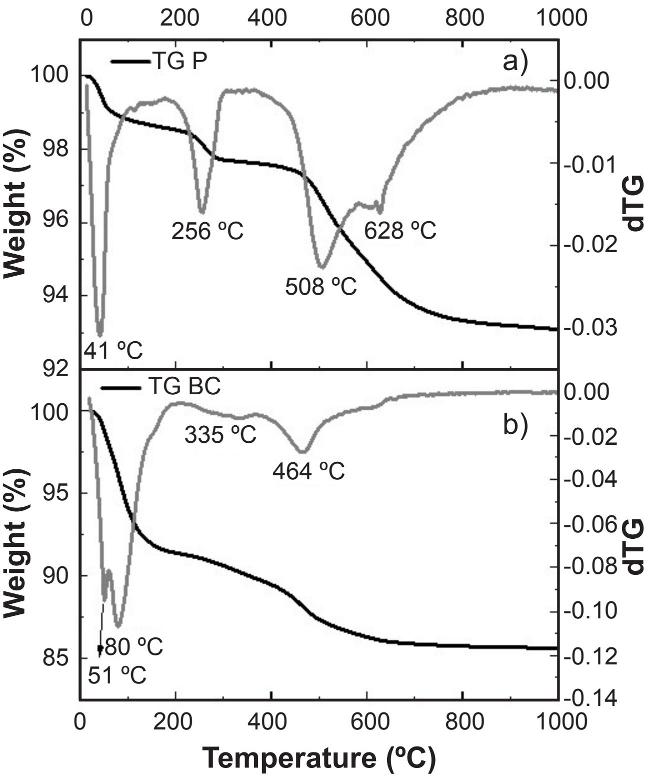

Figure 4: Curves of thermogravimetric analysis (TG) of the raw materials: a) P; and b) BC. Derivative curves (DTG) are plotted as well on the right axis.

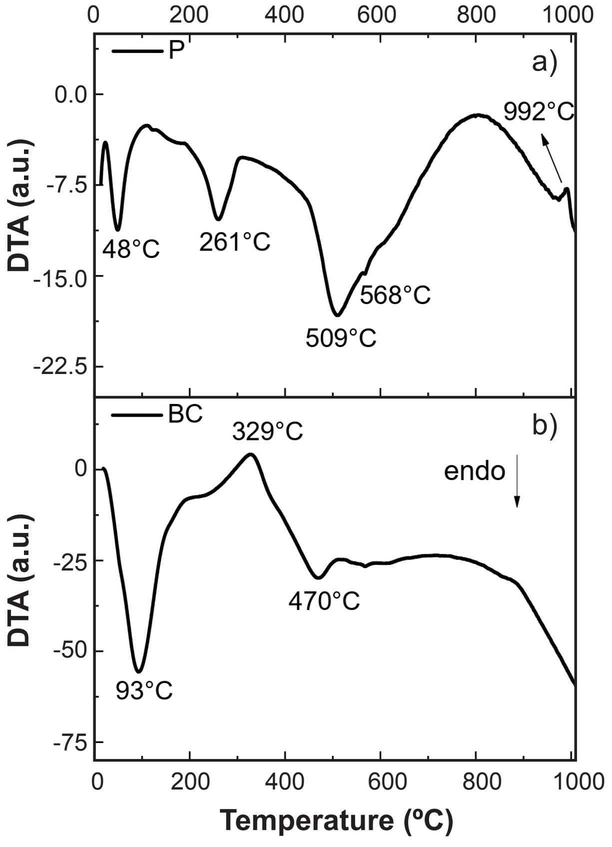

Figure 5: Curves of differential thermal analysis (DTA) of the raw materials: a) P; and b) BC.

energy involved in the decomposition of calcite ($CaCO_3$) is not detectable by this technique when the content is so low. It would only be detectable by mineralogical analysis on calcined samples, as shown in the next section.

Systematic clay paste characterization

The hydration of the clay pastes was carried out directly from the mixed dry raw materials and the addition of water and manual kneading as in traditional pottery practice. Usually, the pastes are stored and protected for long periods of hydration (months and years). This operation is usually performed for adjusting homogeneity and improve the workability of the pastes [13]. BC is the one that introduces plasticity in the pastes, the finer fractions of P are plastic as well, and the coarse-grains present in P powder plays an anti-plastic or load role. In fact, the coarsest grains are not able to hydrate in the filling and storing [7, 9, 12]. The mass ratio of raw materials in the paste was greater than 9:1 between P:BC, and was empirically adjusted by the potter in the mixing and kneading operation, using the workability of the mixture as a parameter to optimize [7]. The plasticity of BC powder and paste (PP) was studied using the Atterberg method [32]; the results are shown in Table IV. While the BC sample had high plasticity, the PP was of medium plasticity [33], confirming its aptitude for different forming strategies in the plastic state [12, 13].

Table IV - Atterberg parameters of the studied clay pastes.

Sample	Liquid limit (%)	Plastic limit (%)	Plasticity index (%)
Prepared paste (PP)	30.0	18.2	11.8
Barro Chico (BC)	62.0	28.0	34.0

Drying behavior: the workability of the pastes must not be tested with technological or operational objectives, since it was provided by an artisan, who usually uses them for their production. However, we consider it illustrative to report the values of the technological parameters and behaviors. It is well known that the drying of the raw pieces implies a highly critical moment with regard to the production cycle of ceramic pieces [34]. Characterization of the drying behavior of the paste was carried out together with the plasticity parameters; both behaviors allowed to account for the aptitude and specificity of the raw materials for their use in pottery productions. Fig. 6 shows examples of experimentally constructed Bigot curves for the PP sample. In the first place, it should be noted the low water content of the clay paste; this was due to the important fraction of coarse and non-hydrated grains of the Pirka clay; about 18 wt% was the plastic limit, a slight discontinuity was observed in the curve (~1%). Secondly, the low shrinkage, approximately 5% shrinkage on drying, stood out. The critical point of contraction was achieved near 9% humidity; below that humidity, the pieces did not modify their dimension.

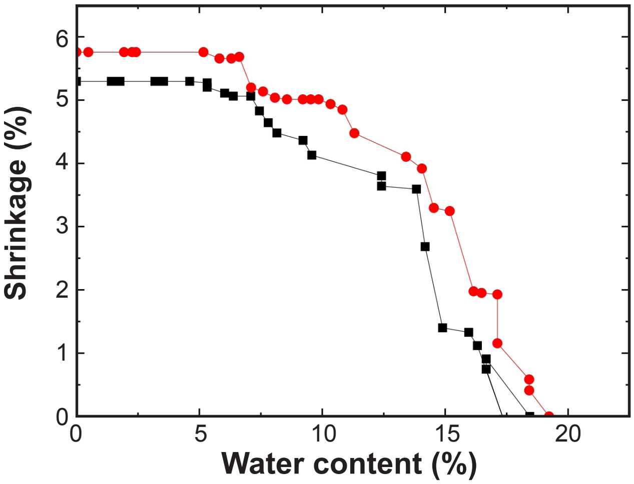

Figure 6: Bigot curves of the PP clay paste.

Clay paste firing behavior: the main heat treatment of the ceramics was carried out with a vertical load wood kiln [13]; in some cases, it was carried out in the open and with guano [12], although this practice has been replaced by wood-firing. Temperature control is usually done empirically, by firing time or kiln color. The atmospheric characteristics of wood-fired kilns are variable and fluctuate between neutral, oxidizing, and somewhat reducing atmospheres, whereas pit-fire-type open-air baking tends to have a strongly reducing and slightly reducing predominance [12, 14]. This section shows a systematic study of the effect of the cooking temperature on the dimension of the paste as a function of the cooking temperature, in an air atmosphere. Fig. 7 shows the reversible dilatometry with successive maximum temperatures; from these tests, a distinctive behavior of the paste was observed. The material treated at 400 °C was easily rehydrated and did not result in a ceramic material; the rest of the samples, fired at higher temperatures, achieved the transformation to ceramic material in an irreversible way and no rehydration was achieved in a simple test. Then the behavior observed for the paste tested in the complete cycle (heating-cooling up to 1000 °C) was as follows: a non-linear growth curve (possibly exponential) up to 550 °C, temperature at which there was a change (acceleration) in the expansion rate of the sample, related to the α-β transformation of quartz (573 °C), then decelerated its growth from that point gradually and the length achieved its maximum in the form of a plateau between 800 and 900 °C. From that temperature, a shrinkage of the piece began up to 1000 °C, the maximum temperature tested, since it is the firing temperature range of this type of ceramic [13]. These growth changes corresponded to the thermochemical processes identified by DTA-TG, that was, the dehydroxylation of clays (450-600 °C), the transformation of quartz (573 °C), and the formation of spinel (SAS, 980 °C); this last process was probably accompanied by a loss of porosity or sintering. In the cooling hemicycle, the shrinkage slope changed around 573 °C, as it passed through the β-α transformation of quartz and shrank almost constantly up to room temperature. The resulting sample from this heat treatment presented a 0.4% enlargement. The cooling slope was lower than the heating slope.

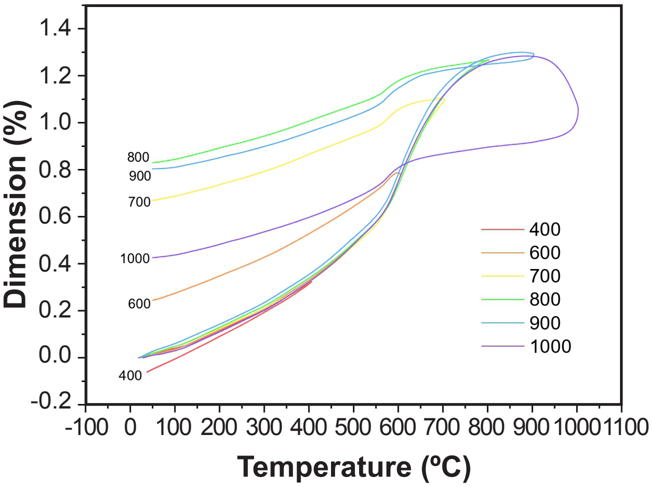

Figure 7: Results of reversible dilatometric analysis of samples prepared from de PP clay paste treated at different maximum temperatures (400, 600, 700, 800, 900, and 1000 °C).

Subsequently, a systematic test was carried out at different maximum temperatures, maintaining the rest of the test conditions; from that test, two firing parameters were constructed: the maximum dimension reached in the cooking cycle (L_m) and the resulting dimension at room temperature after the controlled firing cycle (L_f). These parameters are plotted as a function of the maximum temperature of the cycle in Fig. 8. The expansion of the ceramic tiles during firing reached 1.2% of their dimension. Then they resulted in ceramics with a maximum expansion of 0.83%. Both parameters were parallel, showing a plateau between 700 and 900 °C. The expansion suffered by ceramics during firing was low and allowed rapid firing of these ceramics. Likewise, the possible thermo-elastic stresses typical of an uneven vertical draft kiln or pit firing which present gradients of more than 100 °C, would not result in catastrophic events.

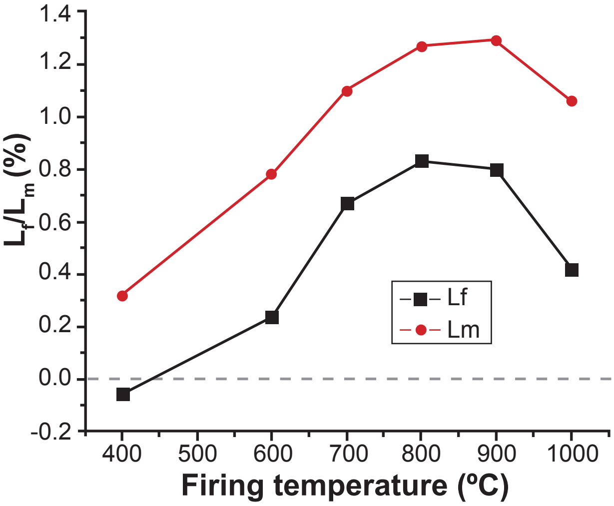

Figure 8: Firing parameters, final shrinkage (L_f), and maximum shrinkage (L_m), of the ceramics fired at different maximum temperatures.

Technological properties of the ceramic

The study included an analysis of the crystalline phases present, a textural characterization based on the immersion method and mercury porosimetry, and a microstructural analysis based on electron microscopy. Finally, the thermal behavior of the ceramic was determined.

Crystalline composition of the fired ceramic: an analysis of the resulting crystalline phases was performed by X-ray diffraction; Fig. 9 shows the diffraction pattern and Table II shows the crystalline phases identified as main and accessory phases. In general, the identified components corresponded to that of ceramics based on similar clays [14, 35], and these were correlated with raw materials composition (BC and P) and the heat treatment. As described, the manufacturing temperature of the ceramics was not exactly known due to the firing method carried out by the producers in wood-fired kilns, without (instrumented-based) temperature control. It is for this reason that the analysis of the present phases can provide strong evidence to identify the firing conditions of these ceramics. In any case, it is to be expected that this temperature exceeds 700 °C and does not exceed 900 °C [14]. It is worth noting the presence of a band centered at 22° (2θ) that corresponded to the presence of an amorphous phase based on silica [36, 37]. The main phase corresponded to quartz, which was present in raw materials. Clay components (Table II) could not be identified, except for the diffraction peaks that corresponded to illite. The other clays underwent thermochemical transformations during ceramic firing, as was observed in the thermal analysis. In the same way, two of the feldspars presented in the mixtures without heat treatment were identified in the ceramic. This fact showed that the firing temperature was below the transformation (melting-fusion) temperatures of these phases. In the same way, the raw material P presented small diffractions corresponding to calcite, which presented a thermal decomposition close to 800 °C [21, 37, 38]. The presence of calcite in the mineralogical composition of the ceramic inferred that, during the manufacturing, heat treatment did not exceed this temperature; however, the re-carbonation of free/active calcium oxide can happen if the chemical conditions are met [39]. Finally, diffraction peaks corresponding to hematite were identified, which were also present in one of the raw materials and evidently did not participate in the thermochemical processes during the firing of the ceramics.

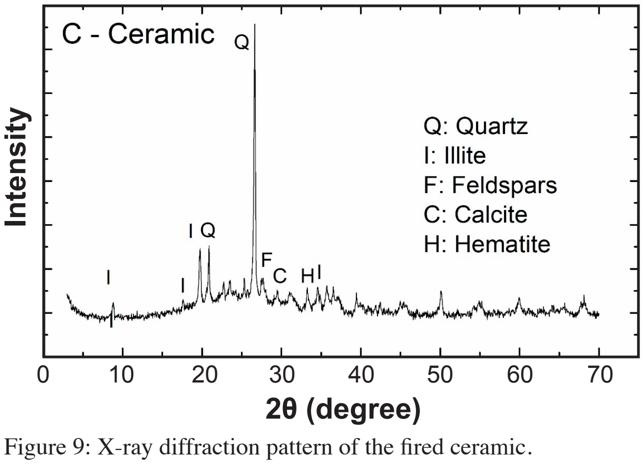

Figure 9: X-ray diffraction pattern of the fired ceramic.

Texture and microstructure of the studied ceramic: the results of the immersion test are shown in Table V, and Fig. 10 shows data on the pore size distribution. Specifically, it can be argued that the ceramic was of porous type [33], and its porosity presented an asymmetric mono-modal distribution below ~0.1 μm. The porosity values were similar to those of many popular everyday ceramics [14], however, the pore size distribution values were remarkably low (below 110 nm).

Table V - Textural parameters of the studied ceramic.

Open porosity (%)	Apparent density (g/cm^3)
19.1 (1.8)	1.99 (0.05)

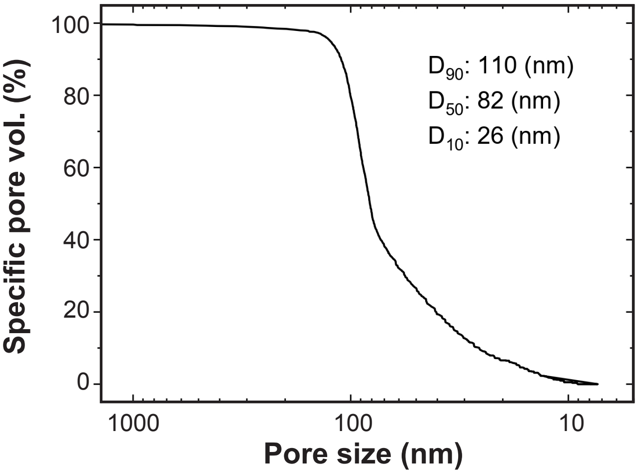

Figure 10: Pore size distribution curve of the studied material.

Fig. 11 shows an SEM image that reveals the microstructure of the ceramic; the structures of the fired clays and accessory minerals are observed, as well as a quartz inclusion (~30 μm) in the center of the image. The microstructure observed corresponded to the porosimetry results evaluated (Fig. 10); no large pores were observed. That is, the porosity of ~20%, evaluated by Archimedes and characterized by mercury intrusion, was constituted by the voids or spaces of interstitial packing of the clay crystals (laminar) and it was not observable at the level of definition. Although they are porous ceramics, the ceramics present a very fine porosity, which gives them excellent technological properties [40].

Dilatometry at 500 °C and possible culinary use: finally, a dilatometric study of the ceramic was carried out in a temperature range typical of domestic culinary use (Fig. 12). It was observed that the ceramic presented a slightly negative coefficient of thermal expansion (-1.6x10^{-6} ºC^{-1}). This distinctive fact gives this ceramic an excellent property

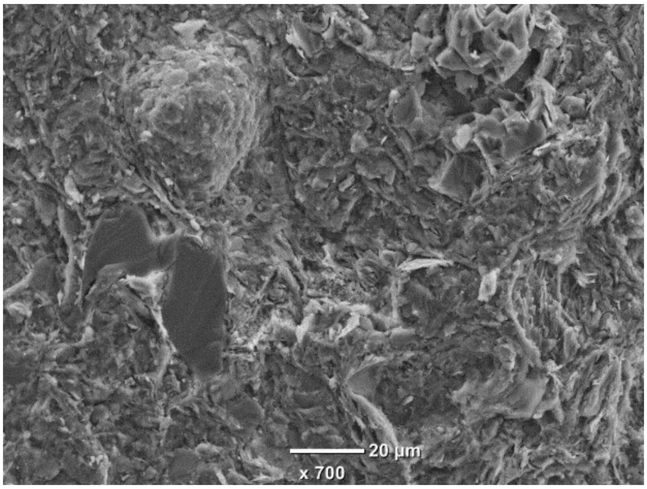

Figure 11: SEM image of the fired ceramic (fractured surface) showing quartz inclusions and a typical clay-sintered microstructure.

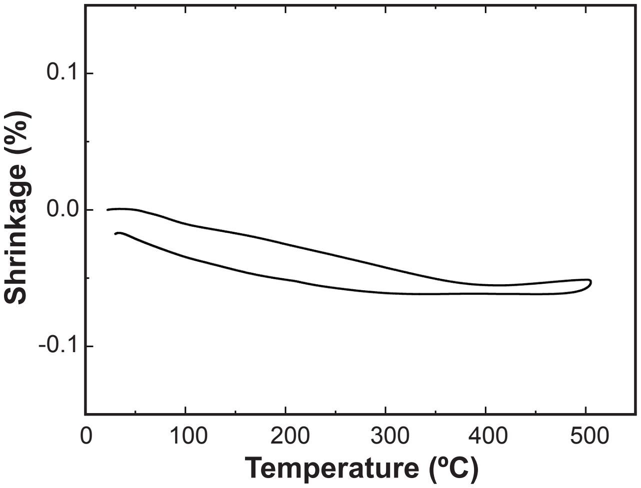

Figure 12: Dilatometric curve of the studied ceramic material in the usage temperature range: room temperature to 500 ºC.

in applications with stresses originating from thermal gradients and thermal shocks, such as culinary applications with direct fire [41, 42] and other applications of high thermomechanical stress [40, 43-45].

DISCUSSION

The Puna is a macro-region with characteristic geo-climatic properties, of which the high altitude above sea level, the low pressure, the dry environment, the little rain, the strong sun, and the high thermal amplitude stand out. Access to fuel was always difficult and was associated with the production of livestock and the use of some local shrubs. Waste wood from other regions of the same province of Jujuy has recently been incorporated as fuel for ceramic production [7]. The availability of clay for ceramic pottery use in the Casira area has allowed the development of this activity. The local clay (Pirka) is a kaolinitic clay of relative refractoriness and high hardness in the stone state; it is expected that this specificity infers distinctive characteristics to the local pottery production. It is worth noting the type of granulometric adaptation used by local potters, who unlike other potters make a coarse crushing of stone clay instead of achieving a fine grain size typical of pottery production below 200 mesh (74 µm). On the contrary, when grinding the clay, a wide grain size distribution that goes from 3 mm to 200 mesh is achieved, making the main component of the formulation with a wide distribution, which in other types of ceramics, such as refractories, would be understood as concrete [46]. The plasticity of the formulation is only incorporated by the finer fractions and by adding a highly plastic clay, like BC, achieving optimal workability with relatively low incorporation of water (<20 wt%). In this way during the forming operations, the potters can advance in height at a relatively fast speed compared to other clay pastes [32, 40, 47, 48].

Then, the drying of the clay pastes is also distinctive; on one hand, the characteristics of the raw materials and the shaping route make the water proportion low; on the other hand, the climatic and geographical conditions of the region result in low-pressure and low or almost no humidity [49-52]. Consequently, the workshops use to dry the pieces in the open air without much protection from the drying rate. The heat treatments are achieved with a remarkable energy economy and using previously the scarce energy resources available locally and now using affordable energy resources in this remote geographical area. The purchase on a scale of by-products of the wood industry of the same province has proven, in recent times, to be a sustainable resource from the economic point of view of the pottery activity. Also noteworthy is the low expansion suffered by ceramic bodies during firing, which facilitates the rapid firing of these ceramics [42, 47, 48, 53]. Subsequently, it is worth highlighting the excellent technological properties of the materials achieved in the Casira pottery workshops, since the texture and microstructure of the ceramics with porosity of less than 20% and pores of submicrometric sizes are remarkable [23]. These characteristics, added to a null (slightly negative) thermal expansion in the range of use (below 500 °C), make Casira ceramics unique in the region and comparable to other important popular ceramic productions [40, 54, 55].

CONCLUSIONS

Several aspects of the ceramic properties and manufacture of high-value ceramic pieces were described and analyzed. The distinctive drying and firing behaviors were described together with the technological properties as well. The evaluated properties inferred and confirmed the suitable conditions for their culinary use and their relationship with some characteristics of the raw materials and the climatic conditions of the region. Finally, we argued that the obtained results, in terms of the chemical, crystal-chemical, microstructural, textural, and thermal characterization of Casira ceramics allowed the establishment of their distinctive properties and also the bases for the traceability of these ceramics which would be of interest about the protection and promotion of this pottery as a cultural heritage of the region.

ACKNOWLEDGMENTS

This work has been supported by the Argentinian funding institutions Consejo Nacional de Investigaciones Científicas y Técnicas (CONICET), Agencia Nacional de Promoción Científica y Tecnológica (ANPCyT, PICT 2016-1193), and Universidad Nacional de La Plata (UNLP, X-904). AP and MFS thank CONICET for the scholarships, NMR is a member of CONICET. The authors would like to express their special gratitude to the people of Casira for their great contribution to the cultural heritage of the region, and especially to the artisans Rubén Mamani, Damián Cruz, Andrea Párraga y Doña Martina, and their families, for providing us with the raw materials, the prepared paste and the ceramic motif of study.

REFERENCES

[1] R. Gil Montero, Rev. Demogr. Hist. **22**, 1 (2004) 185.
[2] R. Gil Montero, Estud. Migrat. Latinoam. **21**, 62 (2007) 43.
[3] M. Beierlein de Gutierrez, Comechingonia Rev. Arqueol. **11**, 1 (2008) 105.
[4] M. Beierlein de Gutierrez, Est. Atacameños **37**, 1 (2009) 51.
[5] F. Ávila, Theoria **14**, 1 (2005) 85.
[6] F. Ávila, Intersec. Antropol. **9** (2008) 197.
[7] C.I. Angiorama, M.J. Pérez Pieroni, M.F. Becerra, M.N. Giusta, Pobl. Soc. **25**, 1 (2008) 5.
[8] M.B. Cremonte, C. Otero, M.S. Gheggi, Relac. Soc. Arg. Antropol. **34** (2009) 75.
[9] K. Menacho, Intersec. Antropol. **8** (2007) 149.
[10] M.N. Tarragó, Intersec. Antropol. **8** (2007) 87.
[11] K. Menacho, Relac. Soc. Arg. Antropol. **26** (2001) 119.
[12] M.J. Pérez Pieroni, Materialidades **2** (2014) 94.
[13] M.J. Pérez Pieroni, Relac. Soc. Arg. Antropol. **40** (2015) 13.
[14] D.A. Santacreu, *Materiality, techniques and society in pottery production: the technological study of archaeological ceramics through paste analysis*, De Guryter, Berlin (2014).
[15] G.E. Barnes, Appl. Clay Sci. **80** (2013) 281.
[16] M. Dondi, Resour. Conserv. Recycl. **133** (2018) 191.
[17] C. Rodriguez-Navarro, E. Ruiz-Agudo, A. Luque, A.B. Rodriguez-Navarro, M. Ortega-Huertas, Am. Mineral. **94**, 4 (2009) 578.
[18] G. Cultrone, C. Rodriguez-Navarro, E. Sebastian, O. Cazalla, M.J. De la Torre, Eur. J. Mineral. **13**, 3 (2001) 621.
[19] K.S.P. Karunadasa, C.H. Manoratne, H.M.T.G.A. Pitawala, R.M.G. Rajapakse, J. Phys. Chem. Solids **134** (2019) 21.
[20] A.P. Luz, M.A.L. Braulio, V.C. Pandolfelli, *Refractory castable engineering*, Göller Verlag, Baden-Baden (2015).
[21] E. Gliozzo, Archaeol. Anthropol. Sci. **12**, 11 (2020) 260.
[22] N.H. Brett, K.J.D. MacKenzie, J.H. Sharp, Q. Rev. Chem. Soc. **24**, 2 (1970) 185.
[23] W.M. Carty, U. Senapati, J. Am. Ceram. Soc. **81**, 1 (1998) 3.
[24] F. Bergaya, G. Lagaly (Eds.), "Handbook of clay science", Elsevier, Amsterdam (2013).
[25] M. Bellotto, A. Gualtieri, G. Artioli, S.M. Clark, Phys. Chem. Miner. **22**, 4 (1995) 207.
[26] A.K. Chakraborty, *Phase transformation of kaolinite clay*, Springer, New Delhi (2014).
[27] L. Andrini, R. Moreira Toja, M.R. Gauna, M.S. Conconi, F.G. Requejo, N.M. Rendtorff, Appl. Clay Sci. **137** (2017) 233.
[28] G.W. Brindley, M. Nakahira, J. Am. Ceram. Soc. **42**, 7 (1959) 314.
[29] A.K. Chakraborty, in *Phase transformation of kaolinite clay*, Springer, New Delhi (2014) 13.
[30] M.S. Conconi, M. Morosi, J. Maggi, P.E. Zalba, F. Cravero, N.M. Rendtorff, Cerâmica **65**, 374 (2019) 227.
[31] K. Okada, N. Otsuka, J. Ossaka, J. Am. Ceram. Soc. **69**, 10 (1986) 11.
[32] F.A. Andrade, H.A. Al-Qureshi, D. Hotza, Appl. Clay Sci. **51**, 1 (2011) 1.
[33] M. Dondi, M. Raimondo, C. Zanelli, Appl. Clay Sci. **96** (2014) 91.
[34] E. Mancuhan, S. Özen, P. Sayan, S.T. Sargut, Dry. Technol. **34**, 13 (2016) 1535.
[35] L.A. Gaspar Junior, A.F.D.C. Varajão, M.H.O. Souza, M.M.T. Moreno, Cerâmica **58**, 347 (2012) 404.
[36] M.S. Conconi, M.R. Gauna, M.F. Serra, G. Suarez, E.F. Aglietti, N.M. Rendtorff, Cerâmica **60**, 356 (2014) 524.
[37] M.F. Serra, M.F. Acebedo, M.S. Conconi, G. Suarez, E.F. Aglietti, N.M. Rendtorff, Ceram. Int. **40**, 1 (2014) 1709.
[38] M.F. Serra, M.S. Conconi, G. Suarez, E.F. Agietti, N.M. Rendtorff, Cerâmica **59**, 350 (2013) 254.
[39] V. Morales-Flórez, A. Santos, I. Romero-Hermida, L. Esquivias, Chem. Eng. J. **265** (2015) 194.
[40] J.M. Skibo, *Understanding pottery function*, Springer, New York (2013) 25.
[41] M. Martinón-Torres, T. Rehren, *Archaeometallurgy in global perspective*, Springer, New York (2014) 107.
[42] M.S. Tite, V. Kilikoglou, G. Vekinis, Archaeometry **43**, 3 (2001) 301.
[43] F.J. Parker, J. Am. Ceram. Soc. **73**, 4 (1990) 929.
[44] M.A. Violini, M.F. Hernández, M. Gauna, G. Suarez, M.S. Conconi, N.M. Rendtorff, Ceram. Int. **44**, 17 (2018) 21470.
[45] I. Yamai, T. Oota, J. Am. Ceram. Soc. **68**, 5 (1985) 273.
[46] N. Sarkar, K.S. Lee, J.G. Park, S. Mazumder, C.G. Aneziris, I.J. Kim, Ceram. Int. **42**, 2 (2016) 3548.
[47] G. Bronitsky, R. Hamer, Am. Antiq. **51**, 1 (1986) 89.
[48] L. Cely-Illera, Rev. Fac. Ing. Un. Antioquia **80** (2016) 31.
[49] S. Oummadi, "Drying behaviour of ceramic green bodies: experimental characterization and numerical

modelling", PhD thesis, Un. Limoges (2019).

[50] S. Korpayev, M. Bayramov, S. Durdyev, H. Hamrayev, Materials **14**, 23 (2021) 7471.

[51] P. Aungatichart, S. Wada, Appl. Clay Sci. **43**, 2 (2009) 182.

[52] H. El Boudour El Idrissi, L. Daoudi, M. El Ouahabi, A. Balo Madi, F. Collin, N. Fagel, Appl. Clay Sci. **129** (2016) 108.

[53] G. Bronitsky, in "Advances in archaeological method and theory", M.B. Schiffer (Ed.), Academic Press, San Diego (1986) 209.

[54] C. Espejel, F. Catalá Roca, *Cerámica popular mexicana*, Blume, Barcelona (1975).

[55] J. Llorens Artigas, J. Corredor-Matheos, F. Catalá Roca, *Cerámica popular española*, Blume, Barcelona (1978).

(Rec. 09/02/2022, Rev. 28/04/2022, 05/06/2022, 30/06/2022, Ac. 04/07/2022)